

Synthesis of PAN with adjustable molecular weight and low polydispersity index (PDI) value via reverse atom transfer radical polymerization

Shuang Li^a, Yazhen Wang^b, Liqun Ma^a, Xueze Zhang^b, Shaobo Dong^b, Li Liu^b, Xilai Zhou^a, Chenglong Wang^b and Zhen Shi^a

^aCollege of Materials Science and Engineering, Qiqihar University, Qiqihar, China; ^bHeilongjiang Provincial Key Laboratory of Polymeric Composite Materials, Qiqihar University, Qiqihar, China

ABSTRACT

The reverse atom transfer radical polymerization (RATRP) of acrylonitrile (AN) was carried out in N, N-dimethylformamide (DMF) with AIBN as initiator, FeCl₃·6H₂O/triphenylphosphine (PPh₃) and FeCl₃·6H₂O/pentamethylde-thylenetriamine (PMDTA) as catalytic systems, respectively. Effect of reaction time and initiator concentration on polymerization rate, molecular weight and molecular weight distribution were investigated in detail. The Fourier transform infrared spectrometer (FTIR) and ¹H nuclear magnetic resonance spectroscopy (¹H NMR) were employed to analyze the chain end of the PAN. Gel permeation chromatography (GPC) was applied to measure the molecular weight and polydispersity index (PDI) of PAN. The polymerization demonstrated a typical pseudo first-order kinetics characteristics as evidenced by the number-average molecular weights (M_n) increasing linearly with monomer conversion; the M_n decreasing with the increasing of the initiator concentration. Meanwhile, the low PDI value (<1.2) indicated the controllability of polymerization.

ARTICLE HISTORY

Received 31 July 2019
Accepted 6 October 2019

KEYWORDS

RATRP; acrylonitrile;
molecular weight;
polydispersity index

1. Introduction

Polyacrylonitrile (PAN) is one of the most significant polymer resins with satisfactory performance in chemical resistance, high hardness and rigidity, good compatibility with certain polar substances, low gas permeability, and it was diffusely applied in many fields [1]. It is well known that low polydispersity index (PDI) is a vital requirement for the synthesis of polyacrylonitrile (PAN) [2]. Traditional free radical polymerization performs poorly in controlling molecular weight and PDI [3,4]. Atom transfer radical polymerization (ATRP) provides a satisfying method to obtain a controllable polymer with prospective molecular weight, low PDI [5–8]. At present, ATRP has been widely used to prepare macromolecules with complex structures such as random, block, graft, cyclic, hyperbranched, dendritic, cross-linked network structures, etc. There is a rapid dynamic balance between dormant species and active species in a typical ATRP, so that the concentration of radicals could maintain at a low degree to control the molecular weight and distribution [9]. However, conventional ATRP has some limitations such as the toxicity of initiator alkyl halide, RX, and the catalyst is sensitive to oxygen and humidity [10–13]. To overcome these shortcomings, the RATRP has been developed. RATRP

was firstly reported by Matyjaszewski [14–16], it subsequently opened up a new field for control/living polymerization and has aroused a hot research. Differing from the ATRP, in the initiation stage of RATRP, it used conventional initiator such as BPO and AIBN [17,18] instead of alkyl halide (RX) and oxidation state transition metal catalysts such as Cu²⁺, Fe³⁺ and Ni²⁺ [19–21] instead of reduction state transition metal catalyst [22–24].

In the past years, a tremendous amount of attempts have been made to develop new initiators and new catalytic systems of RATRP [25–29], there are also many studies have been aimed at finding new solvents and ligands which made an influence of the reactivity [30–32]. Qin [33] reported a RATRP of styrene which was investigated with initiating system, DCDPS/FeCl₃/PPh₃, in which diethyl 2, 3-dicyano-2, 3-diphenylsuccinate (DCDPS) was a hexa-substituted ethane thermal iniferter. Ma [34] et al successfully carried out the RATRP of AN with FeCl₃/acetic acid as a catalytic system. However, the information concerning the regulation and control of the molecular weight by changing the parameters including reaction time, initiator concentration remains limited.

CONTACT Yazhen Wang  yzwang2957@163.com  Heilongjiang Provincial Key Laboratory of Polymeric Composite Materials, 42 Wenhua Street, Jianhua District, Qiqihar 161006, China

© 2019 The Author(s). Published by Informa UK Limited, trading as Taylor & Francis Group.
This is an Open Access article distributed under the terms of the Creative Commons Attribution License (<http://creativecommons.org/licenses/by/4.0/>), which permits unrestricted use, distribution, and reproduction in any medium, provided the original work is properly cited.

Inspired by this issue, in this study, we synthesized the PAN via RATRP with AIBN as initiator, $\text{FeCl}_3 \cdot 6\text{H}_2\text{O}$ /triphenylphosphine (PPh_3) and CuBr_2 /pentamethyldiethylenetriamine (PMDETA) as catalytic systems, respectively. We investigated the effect of reaction time and initiator concentration on molecular weight and aimed at regulate the molecular weight by changing the parameters of RATRP.

2. Experimental section

2.1. Materials

Acrylonitrile, 2,2-azobisisobutyronitrile, ferric chloride ($\text{FeCl}_3 \cdot 6\text{H}_2\text{O}$), triphenylphosphine (PPh_3), CuBr_2 , pentamethyldiethylenetriamine (PMDETA) were bought from Aladdin Chemistry (Shanghai, China), N, N-dimethylformamide (DMF), methanol were supplied by Kermel Chemistry (Tianjin, China). All the chemicals mentioned above were analytical reagent and used without further purification.

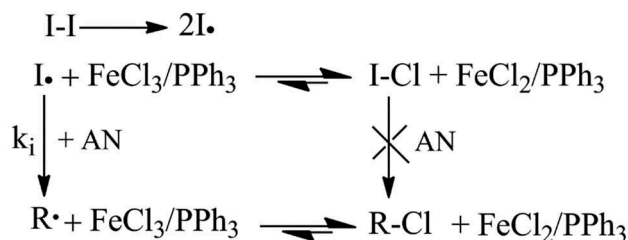
2.2. Polymerization

An example for a general polymerization process was as follows. $\text{FeCl}_3 \cdot 6\text{H}_2\text{O}$, PPh_3 , DMF, AIBN and AN were added to a flask under stirring in that order, $([\text{AN}]_0/[\text{AIBN}]_0/[\text{FeCl}_3 \cdot 6\text{H}_2\text{O}]_0/[\text{PPh}_3]_0 = 500:1.0:1:1)$, the mixture was degassed in vacuum and filled with nitrogen. After undergoing 3 times N_2 -vacuum- N_2 cycles, the sealed flask was charged with N_2 and the polymerization was carried out at 75°C . After a desired time, cooling the flask to terminate the polymerization. The resultant polymer was precipitated in an excess of methanol-water solution (V: V = 1:1), and then filtered and dried at 55°C . The polymerization mechanism was shown in Scheme 1.

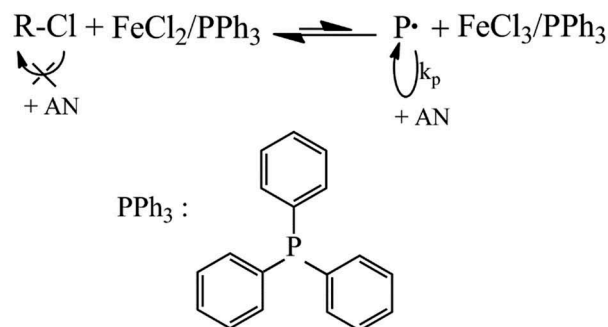
2.3. Characterization

The conversion of AN was measured by gravimetry. M_n and PDI of PAN were determined by GPC system (Wyatt GPC/SEC-MALS, USA). The column system was calibrated with PSt standards ($M_n = 30,000$). DMF was used as an eluent at a flow rate of 0.5 mL/min at 50°C . Samples were filtered with a $0.22 \mu\text{m}$ Organic nylon 66 filter and then were injected manually (syringe volume $V = 1\text{ml}$). FTIR spectroscopy was recorded on a Perkin-Elmer Spectrum 2000 FTIR, the samples was compressed with KBr and measured at room temperature. The spectral range was $4000\text{--}450 \text{ cm}^{-1}$ and the resolution was 4 cm^{-1} . ^1H NMR spectrum was conducted in DMSO at room temperature on a Bruker AV400 NMR spectrometer. Tetramethylsilane was used as internal standard.

Initiation:



Propagation:



Scheme 1. Polymerization mechanism of reverse ATRP of AN and the ligand structure.

3. Results and discussion

3.1. Analysis of chain end

The chain end of the PAN prepared with $\text{FeCl}_3 \cdot 6\text{H}_2\text{O}/\text{PPh}_3$ as catalytic system via RATRP was monitored by the transmittance of FTIR. In Figure 1, the intensity of peak at 2244 cm^{-1} was attributed to the stretching vibration of $\text{C} \equiv \text{N}$, the peaks could be seen at

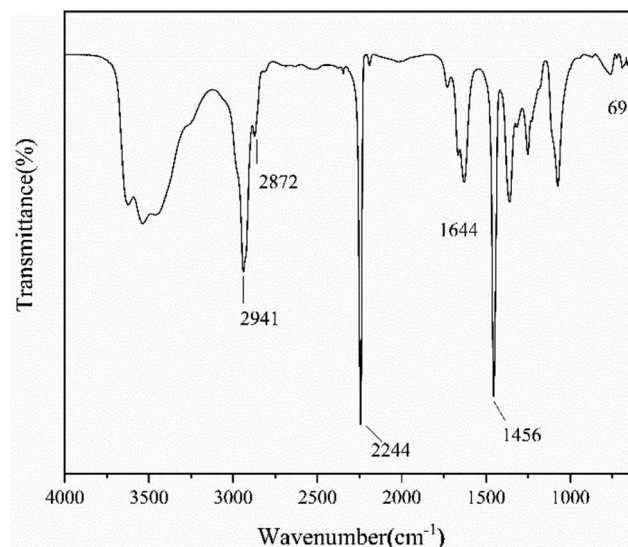


Figure 1. FTIR spectra of PAN synthesized with $\text{FeCl}_3 \cdot 6\text{H}_2\text{O}/\text{PPh}_3$ as catalytic system.

2941 cm^{-1} , 2872 cm^{-1} and 1456 cm^{-1} corresponded to the stretching vibration of $-\text{CH}_2-$ and the bending vibration of C-H, respectively. In addition, the peak at 1644 cm^{-1} related to the unreacted monomeric acrylonitrile of C = C. Merits attention, there is an apparent peak at 691 cm^{-1} which is due to the stretching vibration of C-Cl, it indicated that the polymer chain is terminated with chlorine.

The retention of active functional group in polymer chain ends was further demonstrated by $^1\text{H NMR}$ spectroscopy with DMSO used as the deuterated reagent, the PAN (M_n , GPC = 16,150 g mol^{-1} , $M_w/M_n = 1.137$) provided at the molar ratio of $[\text{AN}]_0/[\text{AIBN}]_0/[\text{FeCl}_3 \cdot 6\text{H}_2\text{O}]_0/[\text{PPh}_3]_0 = 500:1.0:1:1$ under N_2 atmosphere for 6h. As shown in Figure 2. The chemical shift at $\delta = 1.056$ ppm (CH_3- , peak a) was corresponded to the AIBN. The signals at $\delta = 2.041\text{--}2.084$ ppm and $\delta = 3.148$ ppm were attributed to the protons of the methylene groups ($-\text{CH}_2-$, peak b) and hypomethyl proton ($-\text{CH}-$, peak c), respectively. Moreover, the chemical shift at $\delta = 4.35$ ppm was assigned to the protons of $-\text{CH}-$ next to the halogen chain end (peak d), indicating that there are halogen-containing end group in PAN, $\text{CH}_2\text{CCl}(\text{CN})(\text{H})$, which agreed with the report mentioned by Liu's et al [35], the result further proved the unique characteristics of controlled/'living' free-radical polymerization.

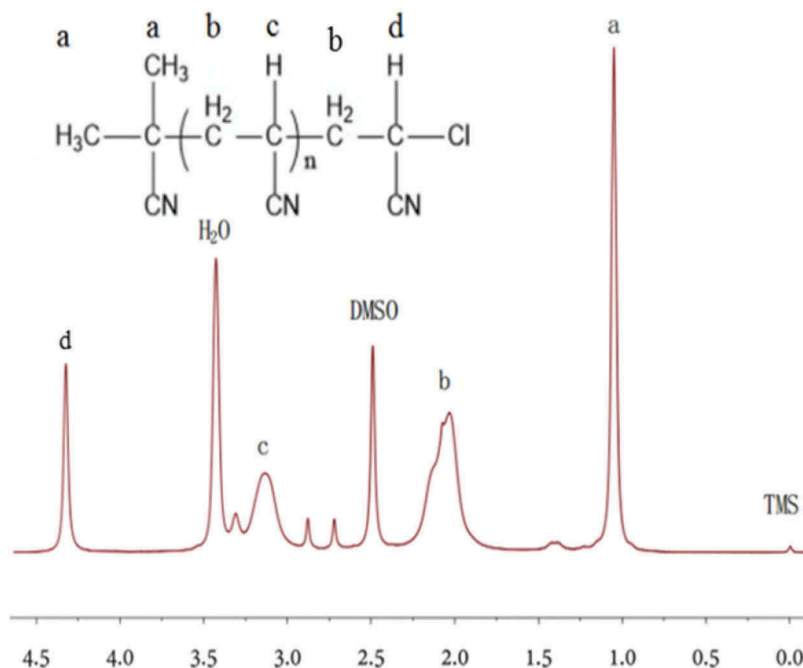


Figure 2. $^1\text{H NMR}$ spectrum of PAN obtained by RATRP the Solvent is DMSO.

$[\text{AN}]_0/[\text{AIBN}]_0/[\text{FeCl}_3 \cdot 6\text{H}_2\text{O}]_0/[\text{PPh}_3]_0 = 500:1.0:1:1$, $V_{\text{DMF}} = 15$ mL, $T = 75^\circ\text{C}$

3.2. Kinetics of Fe-mediated RATRP of AN

The kinetic plots of $\ln([\text{M}]_0/[\text{M}]_t)$ versus reaction time was displayed in Figure 3. Clearly, a liner relationship of $\ln([\text{M}]_0/[\text{M}]_t)$ versus time was observed. The linear semi-logarithmic kinetics demonstrated that the concentration of active species was constant throughout the

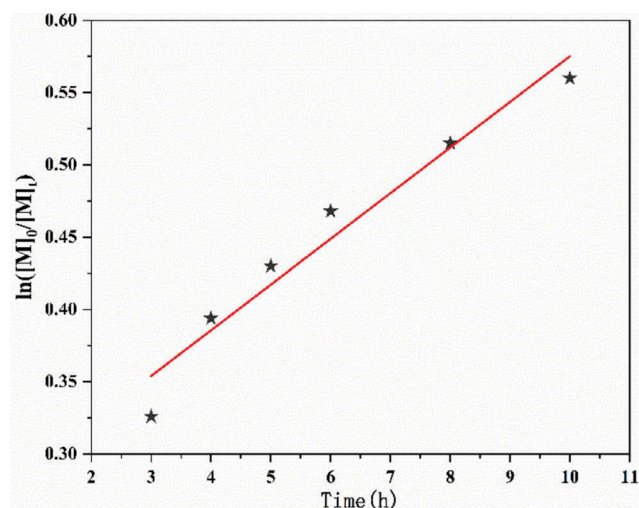


Figure 3. First-order kinetic plot of monomer consumption as a function of time in DMF during reverse ATRP of AN with $[\text{AN}]_0/[\text{AIBN}]_0/[\text{FeCl}_3 \cdot 6\text{H}_2\text{O}]_0/[\text{PPh}_3]_0 = 500:1.0:1:1$, $V_{\text{DMF}} = 15$ mL, $T = 75^\circ\text{C}$.

RATRP process and the polymer chains formed from the biradical termination reactions was negligible. It means that polymerization is conform to first-order with respect to the monomer concentration, and it was regarded as the most important characteristics of a living polymerization. The apparent rate constant (k_p^{app}) was $8.775 \times 10^{-6} \text{ s}^{-1}$ determined from the slope of the kinetic plot. Furthermore, from Figure 3, we can see that the polymerization rate at initial stage was faster than the rate at the latter stage. It could be related to the fact that the initiator AIBN has a higher decomposition rate constant at 75°C so that the greater part of AIBN was decomposed in a shorter polymerization duration [10,36].

The evolution of $M_{n,\text{GPC}}$ and molecular weight distribution (M_w/M_n) with conversion were plotted in Figure 4. The $M_{n,\text{GPC}}$ increased linearly with monomer conversion. In addition, lower M_w/M_n in range of 1.10–1.20 was observed throughout the entire polymerization. Figure 5 exhibited the GPC traces of the PAN with different reaction time. It can be seen that a clean peak shift of low molecular weight polymerization to the high-molecular weight polymerization [22,37]. The monomodal and narrow GPC curve of the chain extended PAN proved the 'living' characteristics of RATRP.

3.3. Effect of initiator concentration on RATRP of AN

The concentration of initiator (AIBN) considerably affects the radical polymerization. In order to probe the role of initiator in polymerization process of AN, the RATRP of AN with different concentrations of AIBN was carried out and the results were shown in Table 1. As shown, with the

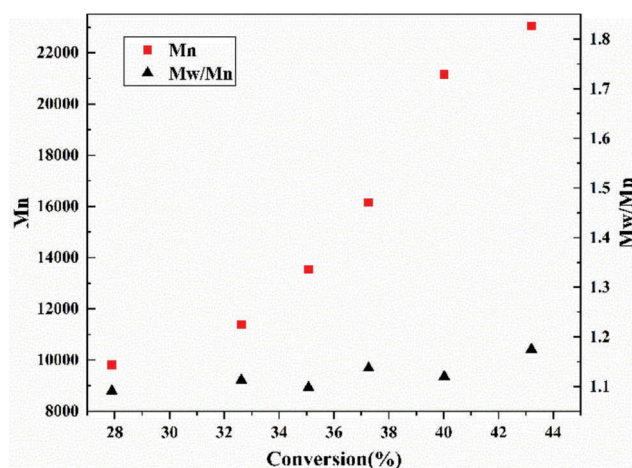


Figure 4. $M_{n,\text{GPC}}$ and PDI versus the conversion for RATRP of AN with $[\text{AN}]_0/[\text{AIBN}]_0/[\text{FeCl}_3 \cdot 6\text{H}_2\text{O}]_0/[\text{PPh}_3]_0 = 500:1.0:1:1$ $V_{\text{DMF}} = 15 \text{ mL}$, $T = 75^\circ\text{C}$.

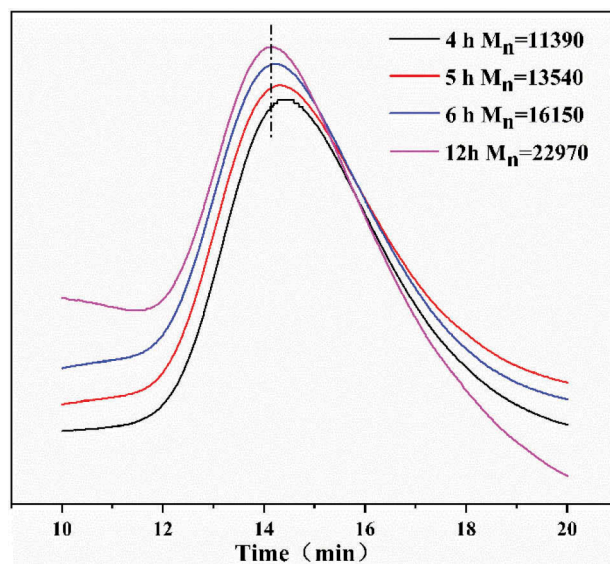


Figure 5. Evolution of GPC traces for PAN synthesized via RATRP with different reaction time. $[\text{AN}]_0/[\text{AIBN}]_0/[\text{FeCl}_3 \cdot 6\text{H}_2\text{O}]_0/[\text{PPh}_3]_0 = 500:1.0:1:1$ $V_{\text{DMF}} = 15 \text{ mL}$, $T = 75^\circ\text{C}$.

increasing of the molar ratio of AN to AIBN from 500:0.5 to 500:1.5, the monomer conversion increased obviously. The monomer conversion was 23.66% after 6h when the $[\text{AN}]:[\text{AIBN}]$ value equals to 500:0.5, the monomer conversion reached 82.8% within the identical polymerization time when the $[\text{AN}]:[\text{AIBN}]$ value equals to 500:1.5. Moreover, as shown in Figure 6(a), the polymerization rate increasing with the molar ratio, $\ln([M]_0/[M]_t)$ was linear with time and the linear coefficients were 0.939, 0.976 and 0.998, respectively, the result was correspond with the first-order dynamics. As shown in Figure 6(b), the M_n (GPC) value decreased with the increasing amount of initiator. Concerning the PDI, it showed a tendency to broaden with the increase of the concentration of AIBN even though it maintained within a narrow range. This can be attributed to the increase in the amount of free radicals with the increasing concentrations of AIBN [38].

Table 1. The effect of increased initiator concentration on RATRP of AN.

Entry	R^a	Time (h)	Conv. (%) ^b	M_n (g/mol) ^c	M_w/M_n^c
1	500: 0.5: 1: 1	3	12.16	11,470	1.017
2	500: 1.0: 1: 1	3	27.90	9820	1.091
3	500: 1.5: 1: 1	3	35.69	9328	1.165
4	500: 0.5: 1: 1	4	13.81	12,810	1.094
5	500: 1.0: 1: 1	4	32.62	11,390	1.113
6	500: 1.5: 1: 1	4	40.16	9958	1.153
7	500: 0.5: 1: 1	5	19.26	14,020	1.010
8	500: 1.0: 1: 1	5	35.07	13,540	1.098
9	500: 1.5: 1: 1	5	44.68	10,740	1.151
10	500: 0.5: 1: 1	6	23.66	18,170	1.122
11	500: 1.0: 1: 1	6	37.26	16,150	1.137
12	500: 1.5: 1: 1	6	48.60	12,090	1.147

^a $R = [\text{AN}]_0/[\text{AIBN}]_0/[\text{FeCl}_3 \cdot 6\text{H}_2\text{O}]_0/[\text{PPh}_3]_0 = 500:0.5:1:1/500:1.0:1:1/500:1.5:1:1$, $V_{\text{DMF}} = 15 \text{ mL}$, $T = 75^\circ\text{C}$

^b Determined by gravimetric method; ^c Determined by GPC in DMF.

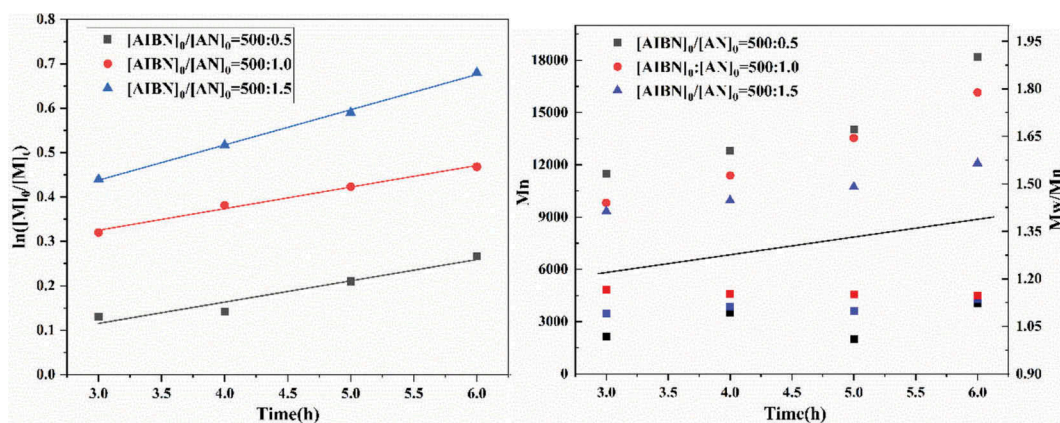


Figure 6. Effect of initiator molar ratio on RATR of AN. (a) $\ln([M]_0/[M]_t)$ as a function of time. (b) M_n and M_w/M_n of PAN versus Reaction time. $[AN]_0/[AIBN]_0/[FeCl_3 \cdot 6H_2O]_0/[PPh_3]_0 = 500:0.5:1:1/500:1.0:1:1/500:1.5:1:1$ $V_{DMF} = 15$ mL, $T = 75^\circ C$.

3.4. RATR of AN with different catalytic systems

In order to research the effect of catalytic system on RATR of AN, the polymerization were conducted by varying the catalytic system. The following catalytic systems were investigated in the study: $FeCl_3 \cdot 6H_2O$ as catalyst, PPh_3 as ligand; $FeCl_3 \cdot 6H_2O$ as catalyst, PMDETA as catalyst. And the experimental data of RATR of AN with different catalytic systems were given in Table 2, whether the polymerization catalyzed by $FeCl_3 \cdot 6H_2O/PPh_3$ or $FeCl_3 \cdot 6H_2O/PMDETA$, the polymers synthesized via RATR both have a low PDI value (<1.2). Comparing with $FeCl_3 \cdot 6H_2O/PPh_3$, $FeCl_3 \cdot 6H_2O/PMDETA$ catalyzed RATR of AN showed a greater conversion and molecular weight in the same reaction time, which proved that the catalytic activity of the transition metal complexes of $FeCl_3 \cdot 6H_2O$ and PPh_3 is higher than that of the transition metal complexes of $FeCl_3 \cdot 6H_2O$ and PMDETA. We can see the plots of monomer conversion and $\ln([M]_0/[M]_t)$ versus reaction time in Figure 7, obviously, both of the RATR catalyzed by $FeCl_3 \cdot 6H_2O/PPh_3$ and $FeCl_3 \cdot 6H_2O/PMDETA$ catalytic system, the linear semi-logarithmic kinetics were observed, and the apparent rate constant (k_p^{app}) were $1.283 \times 10^{-5} s^{-1}$ and

$9.083 \times 10^{-6} s^{-1}$, respectively. The liner relationship of $\ln([M]_0/[M]_t)$ versus time was conform to first-order, confirming the controllability of the controlled/living' polymerization as well.

Conclusion

RATR using AIBN/ $FeCl_3 \cdot 6H_2O/PPh_3$ and AIBN/ $FeCl_3 \cdot 6H_2O/PMDETA$ system has been carried out for AN in DEM successfully. 1H NMR and GPC were employed to analysis of chain end, and confirmed high chlorine chain-end structure of the PAN obtained by RATR. The RATR of AN obeyed the first-order kinetics, indicated that the concentration of active radical species throughout the process of PATRP was approximate constant, and the apparent rate constant (k_p^{app}) was $8.775 \times 10^{-6} s^{-1}$. The M_n increased with increasing concentrations of initiator AIBN and maintained M_w/M_n within a narrow range. Both of the polymerization catalyzed by $FeCl_3 \cdot 6H_2O/PPh_3$ and $FeCl_3 \cdot 6H_2O/PMDETA$ showed a satisfactory controllability, while the catalytic performance of $FeCl_3 \cdot 6H_2O/PMDETA$ was better than $FeCl_3 \cdot 6H_2O/PPh_3$, because of the polymer synthesized in AIBN/ $FeCl_3 \cdot 6H_2O/PMDETA$ system has a higher molecular weight than

Table 2. RATR of AN with three catalytic systems: $FeCl_3 \cdot 6H_2O/PPh_3$, $FeCl_3 \cdot 6H_2O/PMDETA$ and $CuBr_2/PMDETA$.

Entry	Catalytic systems (catalyst/ligand)	Time (h)	Conv. (%) ^a	M_n (g/mol) ^b	M_w/M_n ^b
1	$FeCl_3 \cdot 6H_2O/PPh_3$	3	27.90	9820	1.091
2	$FeCl_3 \cdot 6H_2O/PMDETA$	3	31.55	16,560	1.182
3	$FeCl_3 \cdot 6H_2O/PPh_3$	4	32.62	11,390	1.113
4	$FeCl_3 \cdot 6H_2O/PMDETA$	4	34.45	18,220	1.156
5	$FeCl_3 \cdot 6H_2O/PPh_3$	5	35.07	13,540	1.098
6	$FeCl_3 \cdot 6H_2O/PMDETA$	5	35.63	20,890	1.166
7	$FeCl_3 \cdot 6H_2O/PPh_3$	6	37.26	16,150	1.137
8	$FeCl_3 \cdot 6H_2O/PMDETA$	6	38.04	23,090	1.122

^a Determined by gravimetric method

^b Determined by GPC in DMF.

$[AN]_0/[AIBN]_0/[FeCl_3 \cdot 6H_2O]_0/[PPh_3]_0$ or $[PMDETA]_0 = 500:1.0:1:1$, $V_{DMF} = 15$ mL, $T = 75^\circ C$.

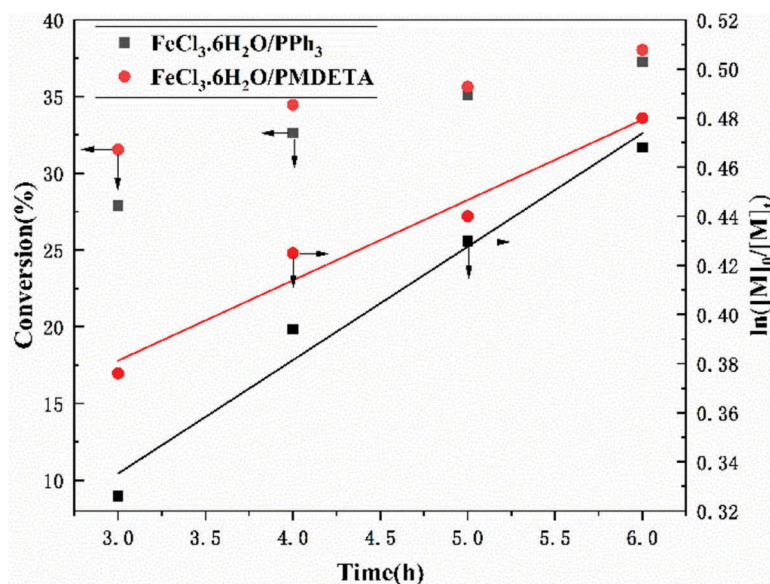


Figure 7. Plots of monomer conversion and $\ln([M]_0/[M]_t)$ versus reaction time for RATRP of AN. $[AN]_0/[AIBN]_0/[FeCl_3 \cdot 6H_2O]_0/[PPh_3]_0$ ($[AN]_0/[AIBN]_0/[FeCl_3 \cdot 6H_2O]_0/[PMDETA]_0$) = 500:1.0:1:1, V_{DMF} = 15 mL, T = 75 °C.

that synthesized in AIBN/ $FeCl_3$ / PPh_3 in the same reaction time. Based above, we can accurately synthesize polymers with a predetermined molecular weight by changing the parameters such as reaction time and initiator concentration.

Disclosure statement

No potential conflict of interest was reported by the authors.

Funding

This work was supported by the National Natural Scientific Foundation of China [Grant No:21376127], the Fundamental Research Funds in Heilongjiang Provincial Universities (Plant food processing technology specialty subject project No: YSTSXK201860), the Fundamental Research Project in Heilongjiang Provincial Education Department [Key projects of science and engineering No:135209102], the Fundamental Research Funds in Heilongjiang Provincial Universities [Grant No:135309110], the Qiqihar City Science and Technology Bureau Project (GYGY-201601) and the Graduate Innovation Research Project of Qiqihar University (YJSCX2018-ZD19).

ORCID

Shuang Li  <http://orcid.org/0000-0001-7275-0730>

References

[1] Matyjaszewski K, Jo SM, Paik HJ, et al. Synthesis of well-defined polyacrylonitrile by atom transfer radical polymerization. *Macromolecules*. 1997;30(20):6398–6400.

[2] Wan LS, Xu ZK, Huang XJ, et al. Copolymerization of acrylonitrile with N-vinyl-2-pyrrolidone to improve the hemocompatibility of polyacrylonitrile. *Polymer*. 2005;46(18):7715–7723.

[3] Grishin ID, Kurochkina DY, Grishin DF. Radical polymerization of acrylonitrile under the action of catalytic systems based on zero-valent copper. *Russ J Appl Chem*. 2015;88(8):1275–1281.

[4] Wiles KB, Bhanu VA, Pasquale AJ, et al. Monomer reactivity ratios for acrylonitrile–methyl acrylate free-radical copolymerization. *J Polym Sci Part A Polym Chem*. 2004;42(12):2994–3001.

[5] Wang JS, Matyjaszewski K. Controlled/“living” radical polymerization. atom transfer radical polymerization in the presence of transition-metal complexes. *J Am Chem Soc*. 1995;117:5614.

[6] Shi GY, Sun JT, Pan CY. Well-defined miktocycle eight-shaped copolymers composed of polystyrene and poly(ϵ -caprolactone): synthesis and characterization. *Macromol Chem Phys*. 2011;212(12):1305–1315.

[7] Matyjaszewski K. Atom transfer radical polymerization (ATRP): current status and future perspectives. *Macromolecules*. 2012;45(10):4015–4039.

[8] Siegwart DJ, Oh JK, Matyjaszewski K. ATRP in the design of functional materials for biomedical applications. *Prog Polym Sci*. 2012;37(1):18–37.

[9] Chi C, Sun B, Zhou N, et al. Anticoagulant polyurethane substrates modified with poly(2-methacryloyloxyethyl phosphorylcholine) via SI-RATRP. *Colloids Surf B Biointerfaces*. 2018;163:301–308.

[10] Liang EX, Zhong M, Hou ZH, et al. Photoinduced ATRP of acrylonitrile with aniline as photoinitiator. *J Macromol Sci Part A*. 2016;53(4):210–214.

[11] Matyjaszewski K, Spanswick J. Controlled/living radical polymerization. *Mater Today*. 2005;8:26–33.

[12] Yue GQ, Liu C, Wang DZ, et al. Nano-sized Li–Fe composite oxide prepared by a self-catalytic reverse atom

- transfer radical polymerization approach as an anode material for lithium-ion batteries. *Mater Res Bull.* **2010**;45(9):1319–1323.
- [13] Zhou W, Chen H, Liang Y, et al. Synthesis of poly (methyl methacrylate) via reverse atom transfer radical polymerization catalyzed by FeCl_3 /lactic acid. *J Appl Polym Sci.* **2009**;114(3):1593–1597.
- [14] Wang JS, Matyjaszewski K. "Living"/controlled radical polymerization. transition-metal-catalyzed atom transfer radical polymerization in the presence of a conventional radical initiator. *Macromolecules.* **1995**;28(22):7572–7573.
- [15] Xia JH, Matyjaszewski K. Controlled/"living" radical polymerization. homogeneous reverse atom transfer radical polymerization using AIBN as the initiator. *Macromolecules.* **1997**;30:7692.
- [16] Moustafa AF, Fang Z, Kennedy JP. Novel polyisobutylene stars. xxviii. a star block comprising three poly (isobutylene-*b*-acrylonitrile) arms radiating from an aromatic core: synthesis and characterization*. *Polym Bull.* **2002**;48(3):225–232.
- [17] Saikia PJ, Hazarika AK, Baruah SD. Iron(III)-mediated ATRP systems of *N*-docosyl acrylate with AIBN and BPO. *Polym Bull.* **2013**;70(5):1483–1498.
- [18] Chen M, Sun F, Xu W, et al. Polymerization of MMA by RATRP in the confined space of polyHIPEs with varied internal phase contents. *J Mater Sci.* **2016**;51(11):5113–5121.
- [19] Zhou H, Chen M, Sun F, et al. Reverse atom transfer radical polymerization of methyl methacrylate in the modified mesoporous SBA-15. *Polym Mater Sci Eng.* **2017**;33(7):17–22.
- [20] Wang Z, Pan X, Yan J, et al. Temporal control in mechanically controlled atom transfer radical polymerization using low ppm of Cu catalyst. *ACS Macro Lett.* **2017**;6(5):546–549.
- [21] Zhou YN, Guo JK, Li JJ, et al. Photoinduced iron(III)-mediated ATRP with in-situ generated initiator: mechanism and kinetics studies. *Ind Eng Chem Res.* **2016**;55(39):10235–10242.
- [22] Hou C, Qu R, Liu J, et al. Reverse ATRP of acrylonitrile with diethyl 2,3-dicyano-2,3-diphenyl succinate/ FeCl_3 /iminodiacetic acid. *Polymer.* **2006**;47(5):1505–1510.
- [23] Sun FM, Xu WF, Chen MS, et al. Polymerization of MMA in polyhypes by RATRP. *J Polym Res.* **2014**;21(12):610.
- [24] Jin SX, Zhou NL, Xu D, et al. Synthesis and anticoagulation activities of polymer/functional graphene oxide nanocomposites via reverse atom transfer radical polymerization (RATRP). *Colloids Surf B Biointerfaces.* **2013**;101:319–324.
- [25] Hou C, Qu R, Ji C, et al. Synthesis of polyacrylonitrile via reverse atom transfer radical polymerization (RATRP) initiated by diethyl 2,3-dicyano-2,3-diphenylsuccinate, FeCl_3 , and triphenylphosphine. *Poly Int.* **2010**;55(3):326–329.
- [26] Zhang W, Yang J, Li B, et al. Reverse atom transfer radical polymerization of styrene in microemulsions catalyzed by CuBr_2 /Bpy. *Polym Sci.* **2013**;55(11–12):551–555.
- [27] Wu Y, Wan G, Xu J, et al. Reverse atom transfer radical emulsion polymerization of styrene and butyl acrylate catalyzed by iron complexes. *Adv Polym Technol.* **2013**;32(4):21364.
- [28] Zhu G, Zhang L, Pan X, et al. Facile soap-free miniemulsion polymerization of methyl methacrylate via reverse atom transfer radical polymerization. *Macromol Rapid Commun.* **2012**;33(24):2121–2126.
- [29] Wang J, Jia P, Pan K, et al. Functionalization of polyacrylonitrile nanofiber mat via surface-initiated atom transfer radical polymerization for copper ions removal from aqueous solution. *Desalin Water Treat.* **2015**;54(10):2856–2867.
- [30] Qin DQ, Qin SH, Qiu KY. Living/controlled radical polymerization of styrene with a new initiating system: DCDPS/ FeCl_3 /PPh₃. *J Polym Sci Part A Polym Chem.* **2015**;38(1):101–107.
- [31] Wang G, Wu H. Microwave-assisted controlled copolymerization of styrene and acrylonitrile catalyzed by FeCl_3 /isophthalic acid. *Polym Bull.* **2011**;67(9):1809–1821.
- [32] Hou C, Qu R, Ji C, et al. Reverse ATRP process of acrylonitrile in the presence of ionic liquids. *J Polym Sci Part A Polym Chem.* **2008**;46(8):2701–2707.
- [33] Li N, Lu J, Xu Q, et al. Reverse atom transfer radical polymerization of mma via immobilized catalysts in imidazolium ionic liquids. *J Appl Polym Sci.* **2008**;103(6):3915–3919.
- [34] Ma J, Chen H, Zong G, et al. FeCl_3 /acetic acid-mediated reverse atom transfer radical polymerization of acrylonitrile. *J Macromol Sci Part A.* **2010**;47(11):1075–1079.
- [35] Liu XD, Ni Y, Wu J, et al. A sustainable photocontrolled ATRP strategy: facile separation and recycling of visible light catalyst fac-[Ir(ppy)₃]. *Polym Chem.* **2018**;9(5):584–592.
- [36] Liu XH, Wang J, Zhang FJ. et al. Copper-mediated initiators for continuous activator regeneration atom transfer radical polymerization of acrylonitrile. *J Polym Sci Part A Polym Chem.* **2012**;50(20):4358–4364.
- [37] Yu YH, Liu XH, Jia D. et al. "Nascent" Cu(0) nanoparticles-mediated single electron transfer living radical polymerization of acrylonitrile at ambient temperature. *J Polym Sci Part A Polym Chem.* **2013**;51(6):1468–1474.
- [38] Zhang L, Cheng Z, Shi S, et al. AGET ATRP of methyl methacrylate catalyzed by FeCl_3 /iminodiacetic acid in the presence of air. *Polymer.* **2008**;49(13–14):3054–3059.